

All about baryons: revisiting SIDM predictions at small halo masses

A.Bastidas Fry¹, F.Governato^{1*}, A.Pontzen², T.Quinn¹, M.Tremmel¹, L.Anderson¹,
H.Menon³, A. M.Brooks⁴ and J.Wadsley⁵

¹*Astronomy Department, University of Washington, Box 351580, Seattle, WA, 98195-1580*

²*UCL, Department of Physics & Astronomy, Gower Place, London WC1E 6BT, UK*

³*Department of Computer Science, University of Illinois at Urbana-Champaign, USA*

⁴*Dept. of Physics & Astronomy Rutgers Univ. 136 Frelinghuysen Rd, Piscataway, NJ 08854*

⁵*Dept. of Physics and Astronomy, McMaster Univ., Hamilton, Ontario, L8S 4M1, Canada*

Revised version April 2015; In original form Dec 2014

ABSTRACT

We use cosmological hydrodynamic simulations to consistently compare the assembly of dwarf galaxies in both Λ dominated, Cold (CDM) and Self-Interacting (SIDM) dark matter models. The SIDM model adopts a constant cross section of $2 \text{ cm}^2/\text{g}$, a relatively large value to maximize its effects. These are the first SIDM simulations that are combined with a description of stellar feedback that naturally drives potential fluctuations able to create dark matter cores. Remarkably, SIDM fails to significantly lower the central dark matter density within the central 500pc at halo peak velocities $V_{\text{max}} < 30 \text{ km s}^{-1}$. This is due to the fact that the central regions of very low-mass field halos have relatively low central velocity dispersion and densities, leading to time scales for SIDM collisions greater than a Hubble time. CDM halos with $V_{\text{max}} < 30 \text{ km s}^{-1}$ have inefficient star formation, and hence weak supernova feedback. At a fixed $2 \text{ cm}^2/\text{g}$ SIDM cross section, the DM content of very low mass CDM and SIDM halos differs by no more than a factor of two within 100-200pc. At larger halo masses ($\sim 10^{10} M_{\odot}$), the introduction of baryonic processes creates field dwarf galaxies with dark matter cores and central DM+baryon distributions that are effectively indistinguishable between CDM and SIDM. Both models are in broad agreement with observed Local Group field galaxies across the range of masses explored. To significantly differentiate SIDM from CDM at the scale of faint dwarf galaxies, a velocity dependent cross section that rapidly increases to values larger than $2 \text{ cm}^2/\text{g}$ for halos with $V_{\text{max}} < 25\text{-}30 \text{ km s}^{-1}$ needs to be introduced.

Key words: Galaxies: formation – Cosmology – dark matter, Galaxies: dwarf.

1 INTRODUCTION

In this paper we use high resolution SPH + N-Body cosmological simulations to focus on two main questions: Can we identify a clear difference between Cold Dark Matter and Self-Interacting Dark Matter (CDM and SIDM respectively) predictions for the structural and observable properties of dwarf galaxies? How do the properties of CDM and SIDM halos differ at halo masses below $10^{10} M_{\odot}$, where star formation (SF) becomes very inefficient and the effect of the underlying DM component should dominate?

SIDM was originally introduced as a solution for the so called “core-cusp” problem, the excess of dark matter predicted by the CDM model at the center of field and satellite dwarf galaxies compared to observations (Moore et al. 1999b; Oh et al. 2008; Walker & Peñarrubia 2011; Adams et al. 2014). In the SIDM model dark matter particle collisions isotropize the cores of galaxies and transfer mass outward from the dense central regions of DM halos over

cosmic time scales. This process creates large cores, more spherical halos, and a signature flat radial profile of the DM velocity dispersion (Spergel & Steinhardt 2000; Burkert 2000). A SIDM model with fixed cross section and elastic collisions represents the simplest model in a large class of plausible “dark sector” DM models. However, significantly more complex interactions are possible, including Yukawa potentials (Feng et al. 2009, 2010; Loeb & Weiner 2011), and cooling or atomic dark matter (Cyr-Racine & Sigurdson 2013; Schutz & Slatyer 2015; Buckley et al. 2014). The dynamics of SIDM was first implemented in cosmological simulations as a fluid (Moore et al. 2000) and then as elastic collisions between particles (Spergel & Steinhardt 2000; Burkert 2000; Davé et al. 2001; Colín et al. 2002; Strigari et al. 2007; Martinez et al. 2009; Koda & Shapiro 2011; Vogelsberger et al. 2012).

Numerical studies combined with observations (the ellipticity of galaxy clusters, the abundance of and the core size of field dwarf galaxies) have constrained the cross section of SIDM to be of the order of $\sim 0.1\text{--}1 \text{ cm}^2/\text{g}$ (Loeb & Weiner 2011; Rocha et al. 2013; Peter et al. 2013; Zavala et al. 2013). However, a variable

* E-mail:(FG); fabiog@astro.washington.edu

SIDM cross section (a decreasing function of the DM particles' relative velocity) can preserve the ellipticity and density of galaxy clusters while producing cores in dwarf galaxies (Peter et al. 2013, but see Newman et al. (2013) for evidence for DM cores in clusters). While weakening existing constraints, a variable SIDM cross section is well motivated by “hidden sector” particle physics models (Tulin et al. 2013). Further crucial constraints on large SIDM cross sections (Elbert et al. 2014) come from the necessity of forming cores in very faint galaxies without evaporating the satellites of MW-like halos and galaxy sized halos in clusters as they interact with a dense DM environment (Gnedin & Ostriker 2001; Vogelsberger et al. 2012).

Unfortunately, a large fraction of the astrophysically driven support for non-standard DM models has come so far from simplified simulations that lack the complexities of “baryon physics” and follow only the assembly of the DM component (see the review by Brooks 2014). The necessity to couple a DM model with baryon physics comes from the existence of “bulgeless galaxies”, a problem that requires the removal of low angular momentum gas from galaxies (Binney et al. 2001; van den Bosch et al. 2001; Governato et al. 2010) through feedback processes (Brook et al. 2011). Further motivation for including baryon physics includes the necessity to quench SF in galaxy satellites (Klypin et al. 1999; Moore et al. 1999a; D’Onghia & Burkert 2003), especially if the SIDM power spectrum is similar to CDM at small scales and subhalos survive evaporation (as found by Zavala et al. 2013).

Crucially, analytical and numerical work have shown that feedback lowers the central DM density in galaxies, creating gas outflows and repeated fluctuations in the gravitational potential (Mashchenko et al. 2008; Del Popolo 2009; Governato et al. 2010; Pontzen & Governato 2012; Di Cintio et al. 2014; Teyssier et al. 2013; Velliscig et al. 2014). This results in irreversible energy transfer to the DM (see also review by Pontzen & Governato 2014). These outflows, generated by a bursty SF, have strong observational support (van der Wel et al. 2011; Martin et al. 2012; Lundgren et al. 2012; Domínguez et al. 2014; Geach 2015). Bursty SFH have also been robustly associated with the build up of the stellar content of galaxies in the 10^8 – $10^{10} M_\odot$ range (Tolstoy et al. 2009; Kauffmann 2014). The ability of feedback to dynamically heat the DM can potentially remove the need for SIDM at galactic scales. As a result it is fundamental to identify the unique differences between CDM and SIDM when both models include an explicit treatment of the physics of galaxy formation.

This study is able to follow the evolution of field SIDM halos at masses below $\sim 10^{10} M_\odot$ ($V_{max}^1 < 40 \text{ km s}^{-1}$). This is an important regime as (1) observational data are becoming robust (e.g., Papastergis et al. 2015), and (2) feedback processes become less efficient with declining V_{max} (Governato et al. 2012; Peñarrubia et al. 2012; Di Cintio et al. 2014). The most recent simulations (Madau et al. 2014; Governato et al. 2015; Oñorbe et al. 2015) show core formation when only $10^{5.7-6} M_\odot$ of stars have formed. Also, it is often naively assumed that SIDM will form DM cores at all dwarf masses. However, at these small halo masses the trend of later assembly epoch of the first progenitor (Li et al. 2008), and consequentially lower central densities (Avila-Reese et al. 2005), will affect the timescale and extent of SIDM core formation in field galaxies beyond simple scaling calculations. Furthermore, the relative velocity of a halo and the surrounding DM background is cru-

cial in determining the collision rate, boosting it in small halos (that have intrinsic low σ). Our subset of DM-only simulations is also one of the first to compare very small field and satellite galaxies at similar mass and spatial resolution. The central density of field and satellite dwarfs (that move fast through a dense DM environment) may then be significantly different, but it has not been properly compared yet.

In this work we adopt a constant velocity cross section of $2 \text{ cm}^2/\text{g}$ in the SIDM runs (a relatively large value to maximize its effects) and a common description of SF and feedback in both CDM and SIDM models. The SF and feedback prescriptions have been shown to form CDM galaxies with SF efficiency, photometric, and kinematic properties close to those of real ones (Oh et al. 2011; Munshi et al. 2013; Christensen et al. 2014a; Shen et al. 2014; Brooks & Zolotov 2014). These simulations are the first high resolution simulations to compare the assembly of dwarf galaxies in CDM vs SIDM cosmologies including a description of SF and supernova feedback that creates realistic galaxies while creating DM cores through “DM dynamical heating.” Other recent numerical work (Vogelsberger et al. 2014) focused on small galaxies in SIDM and explored the role played by a variable cross section, however, the feedback recipe implemented in their work does not generate DM cores.

In §2 we describe the simulation and the code used. In §3 we present the results, which are then discussed in §4.

2 METHODOLOGY

2.1 ChaNGA, star formation and bursty feedback with outflows

The simulations were run in a full cosmological context and to a redshift of zero using the N-body Treecode + Smoothed Particle Hydrodynamics (SPH) code CHANGA (Jetley et al. 2008; Quinn et al. 2013; Menon et al. 2014)². CHANGA includes standard physics modules previously used in GASOLINE (Wadsley et al. 2004, 2008; Stinson et al. 2012) including a treatment of metal line cooling, self shielding, cosmic UV background, star formation, “blastwave” SN feedback and thermal feedback from young stars (Stinson et al. 2006, 2012). The SPH implementation includes thermal diffusion (Shen et al. 2010) and eliminates artificial gas surface tension through the use of a geometric mean density in the SPH force expression (Ritchie & Thomas 2001; Governato et al. 2015; Menon et al. 2014). This update better simulates shearing flows with Kelvin-Helmholtz instabilities. For consistency with our previous work comparing CDM and WDM scenarios, we adopted the same feedback and SF parameters as in Governato et al. (2015). A Kroupa IMF is assumed (Kroupa 2001) and the density threshold for SF is set at 100 amu/cm^3 . Limiting star formation to dense gas regions is a realistic approach and concentrates feedback energy (Brook et al. 2012; Christensen et al. 2014b; Agertz & Kravtsov 2014). 100% of SN energy is coupled to the surrounding gas.

¹ where V_{max} is defined as the peak of the rotation curve, with $V_{rot} = (GM/r)^{1/2}$.

² CHANGA is part of the AGORA group, a research collaboration with the goal of compare the implementation of hydrodynamics in cosmological codes (Kim et al. 2014). CHANGA is available here: <http://www-hpcc.astro.washington.edu/tools/changa.html>

Name	Physics	DM/gas particle mass M_\odot	Force Softening (pc)	halo mass range (M_\odot)
h516CDM	SF and DM-only	$1.6 \cdot 10^4 / 3.3 \cdot 10^3$	86	$10^9 - 5 \times 10^{10}$
h516SIDM	SF and DM-only	$1.6 \cdot 10^4 / 3.3 \cdot 10^3$	86	$10^9 - 5 \times 10^{10}$
h2003CDM	SF and DM-only	$0.67 \cdot 10^4 / 1.4 \cdot 10^3$	64	$4 \times 10^8 - 1 \times 10^{10}$
h2003SIDM	SF and DM-only	$0.67 \cdot 10^4 / 1.4 \cdot 10^3$	64	$4 \times 10^8 - 1 \times 10^{10}$
40Thieves-CDM	DM-only	$0.81 \cdot 10^4$	64	$4 \times 10^8 - 2.7 \times 10^{10}$
40Thieves-SIDM	DM-only	$0.81 \cdot 10^4$	64	$4 \times 10^8 - 2.7 \times 10^{10}$
40Thieves-SIDM.hr	DM-only	$0.24 \cdot 10^4$	64	$1.25 \times 10^8 - 2.7 \times 10^{10}$
h148CDM	DM-only	$1.93 \cdot 10^4$	86	$10^9 - 2 \times 10^{12}$
h148SIDM	DM-only	$1.93 \cdot 10^4$	86	$10^9 - 2 \times 10^{12}$

Table 1. SIMULATIONS AND PHYSICS PARAMETERS EXPLORED IN OUR SIMULATIONS. All SIDM runs adopt $\sigma_{SIDM} = 2[\text{cm}^2 \text{g}^{-1}]$. The mass range shows halos with at least 50,000 DM particles within their virial radius. The main halos in each volume are studied with several million particles each. The DM-only subsample is one of the first to simulate a sample of field and satellite halos at similar mass and spatial resolution. This approach allowed us to study the effect of the environment on the DM distribution of the halos in the two populations.

2.2 SIDM Implementation and Analytical Expectations

The SIDM implementation closely follows the standard Monte Carlo approach described in previous works (Davé et al. 2001; Vogelsberger et al. 2012), and here is only briefly summarized, while tests are presented in Appendix A. SIDM interactions are modeled under the assumption that each simulated DM particle represents a patch of DM phase-space density and that the probability of collisions is derived from the collision term in the Boltzmann equation. Collisions are then elastic and explicitly conserve energy and momentum. For a detailed discussion see (Rocha et al. 2013) and also (Yoshida et al. 2000; D’Onghia & Burkert 2003; Kaplinghat et al. 2014). The number of interactions N that occur in a region with local DM density ρ in a time Δt is

$$N = \rho v \sigma_{dm} \Delta t \quad (1)$$

In practice to simulate interactions for discrete N -body DM particles we use equation one as the implied probability for a particle to scatter. This assumption is valid as Δt approaches zero or numerically where Δt is chosen to be much smaller than needed to avoid multiple collisions. At each time step our numerical code calculates the relative velocity and density ρ using the same functional SPH kernel as in hydro calculations of each DM particle in relation to its 32 nearest neighbors. These values are used to calculate the probability that the DM particle interacts with one of its neighbors. Similar to Vogelsberger et al. (2012), a scattering event may occur at each time step between particles i and j if a uniform random variable in the interval (0,1) is less than $P_{ij}/2$ (the probability is divided by two in order to account for the fact that each set of particles are compared to each other twice). While producing similar results, this approach differs slightly from the one adopted in Rocha et al. (2013), where collisions are defined between DM particle pairs and the probability of interaction $P(i|j)$ is explicitly $= P(j|i)$. When a particle collision is detected we isotropically and elastically scatter the particles to random angles.

The interaction cross section σ for all SIDM runs in this work was set to the relatively large value of 2 g/cm^2 , close to the upper limit for constant σ , in order to maximize its effects compared to that of baryon physics. The way in which SIDM reshapes dif-

ferent halos can be readily understood setting $N = 1$ in eq.1 and $v = v_{\text{max}}$ (where $v_{\text{max}} = \max \sqrt{GM(< r)/r}$) to obtain a characteristic maximum timescale on which a given density is stable,

$$\tau_{\text{SI}} = \frac{1}{\rho v_{\text{max}} \sigma_{dm}}. \quad (2)$$

After a collision, the change in momentum is usually enough to fully eject the particle (Kahlhoefer et al. 2014), so dark matter densities must drop over a few τ_{SI} .

One important conclusion to draw from eq.3 is that not every SIDM model will necessarily form significant cores in the smallest halos. *Low halo peak velocities and low central densities (at a fixed radius) may result in τ_{SI} comparable to the lifetime of a halo and therefore in the preservation of cusps.* Another important consequence is that in SIDM the central densities of very small satellite halos could be differentiated from those of their field counterparts by the interaction with the DM halo of a more massive host as the orbital velocity is much higher than the internal velocities of the satellite. We test these analytical predictions in the next section, where we present results of simulations that resolve the internal structure of DM halos smaller than most previous SIDM studies. Observational evidence of DM cores in small field halos where baryonic processes may be inefficient ($V_{\text{max}} < 20\text{-}30 \text{ km s}^{-1}$ and in satellite galaxies (which move at $100\text{-}200 \text{ km s}^{-1}$ in a $\sim 200\text{-}1000 \times \rho_{\text{crit}}$ DM field) can then provide useful lower limits to the SIDM cross section.

3 CDM AND SIDM SIMULATIONS

In all simulations we assumed a Λ dominated cosmology ($\Omega_0 = 0.26$, $\Lambda = 0.76$, $\sigma_8 = 0.77$, $n=0.96$) and used the “zoom-in” technique to achieve high resolution in the regions of interest (Katz & White 1993). The gravitational force spline softening length is in the range 64-86 pc (Power et al. 2003) and the smoothing length for the gas component is allowed to shrink to 0.1 the force softening. Simulations start at $z = 120 - 100$. The combination of simulations (see Table 1) allow us to compare the effects of SIDM and baryon physics on a range covering almost four orders of magnitude in halo masses and a variety of environments from the field to the dense region within the virial radius of a large field disk galaxy.

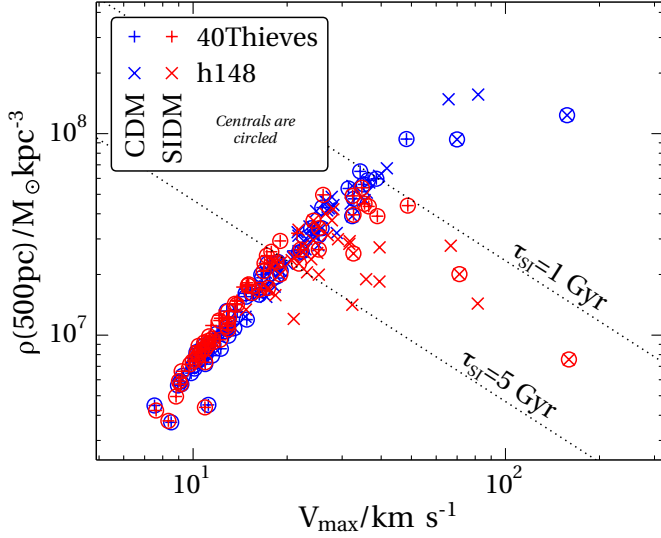


Figure 1. DM-ONLY SIMULATIONS: The DM density measured at 500 pc as a function of halo maximum velocity and dark matter model. Blue crosses: CDM, red crosses: SIDM. Circled symbols correspond to isolated halos, non-circled symbols show the satellites of the MW-sized, h148 halo. At small halo masses the central densities of CDM and SIDM halos do not differ substantially, while at larger velocities/halo masses SIDM-only halos have lower central densities than their CDM-only counterparts. This difference can be understood in terms of the dotted lines which show the maximum timescale τ_{SI} at which collisions are significant in the SIDM case (see text for details). This result shows that fixed cross sections commonly adopted at the scale of larger systems ($0.1\text{--}2\text{ cm}^2/\text{g}$) would not be sufficient to form kpc sized cores in the smallest observable field halos with $V_{\text{max}} < 30\text{ km s}^{-1}$. In the $V_{\text{max}} 30\text{--}60\text{ km s}^{-1}$ range SIDM satellites have central densities lower by a factor two compared to their field counterparts, due to the added boost to SIDM collisions coming from satellites orbiting at high velocity in the dense DM halo of the host.

Cosmological simulations of well resolved halos with mass $< 10^{10} M_{\odot}$ (corresponding to a halo peak velocity $V_{\text{max}} < 30\text{ km s}^{-1}$) are particularly relevant for SIDM, as baryonic effects at these scales should be limited (Governato et al. 2012; Peñarrubia et al. 2012). Based on equation (2), the ability of SIDM to lower the central density of halos depends on the DM ρ and the typical particle velocity, which is lower in less massive halos. Interestingly, previous CDM simulations have suggested that the central density of small mass field halos *decreases* with their halo mass (Avila-Reese et al. 2005; Li et al. 2008). In a SIDM scenario, extending this trend to very small halos could prevent the formation of low density central cores by increasing the time scale of DM-DM collisions.

3.1 DM-only Simulations: Environmental effects and cuspy halos at $V_{\text{max}} < 30\text{ km s}^{-1}$

To study the structure of a significant sample of DM halos in a range of environments we simulated four different regions with the zoomed-in approach (Katz & White 1993). The first three regions (Table 1) are centered on filamentary structures with a density close to average measured inside a sphere of 5 Mpc in radius. The largest one of them is nicknamed ‘The Forty Thieves’ and includes several tens of halos with $V_{\text{max}} < 30\text{ km s}^{-1}$, equivalent to a mass range $10^8\text{--}10^{10} M_{\odot}$, where the minimum mass refers to halos with

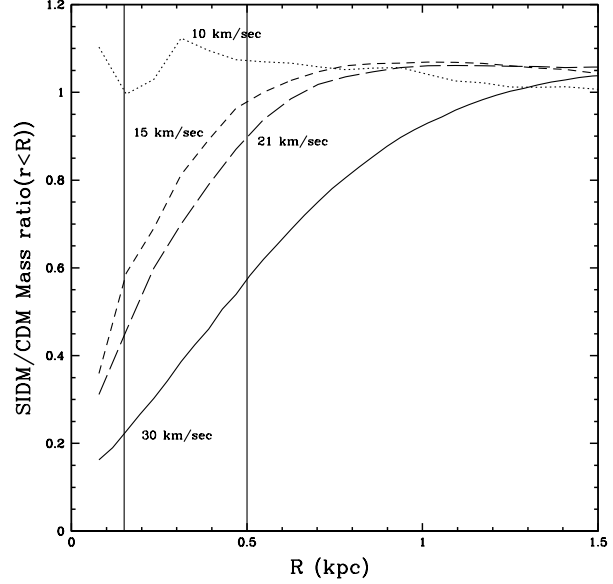


Figure 2. THE RELATIVE DM CONTENT AS A FUNCTION OF RADIUS IN DM-ONLY SIMULATIONS: The ratio of the cumulative DM content measured for a set of small halos over the 0-1.5 kpc radial range (from the 40-Thieves run). Each CDM halo was matched with its ‘twin’ halo in the SIDM simulation. The spline kernel force resolution is 64 pc. Vertical lines mark 150 and 500 pc (2.3 and 5 softening lengths). With our adopted cross section of $2\text{ cm}^2/\text{g}$ small CDM and SIDM become progressively difficult to differentiate, with DM content at a given radius being within a factor of two in the two cosmologies. Detecting such a difference in field dwarfs could require a next generation telescope (M. Walker, private communication). A SIDM with a variable cross section could show a more significant difference compared to CDM.

at least 50,000 DM particles within the virial radius. To complement this dataset, a high resolution simulation of a massive halos and its system of satellites has been included (h148). The halos in this simulation have mass and spatial resolution similar to their ‘40 Thieves’ counterparts and mass and spatial resolution better by factor two compared to recent work Vogelsberger et al. (2012); Zavala et al. (2013). In Appendix 1 we verified that our results and the Monte Carlo implementation of SIDM collisions are not affected by resolution effects.

In Figure 1 we show the density measured at 500 pc (a radius at which the rotation curves of many dwarf galaxies have been resolved, e.g., Oh et al. 2011) for all resolved halos in our h148 (\times) and ‘the 40 Thieves’ ($+$) DM-only simulations as a function of V_{max} . We then over plot lines of fixed τ_{SI} for 1 Gyr and 5 Gyr. SIDM and CDM show identical central DM densities if the typical scale for DM interactions is longer than 5 Gyr. At larger peak velocities (and halo masses) with shorter timescales for interaction, the SIDM densities decrease compared to their CDM counterparts and fall in a valley between the 1 and 5 Gyr lines, matching results from previous works (Rocha et al. 2013; Vogelsberger et al. 2012). In other words, SIDM interactions force the DM density to drop until, going to smaller and smaller halo masses, the interaction timescale rises to a significant fraction of the Hubble time and SIDM (with a $\sigma = 2\text{ cm}^2/\text{g}$) is not effective anymore. Figure 2 shows the SIDM vs CDM ratio of the enclosed mass as a function of radius for paired halos from the ‘40 Thieves’ run. At radii currently tested by observations (100-500 pc), but entirely neglecting baryonic physics, the difference between the two models decreases

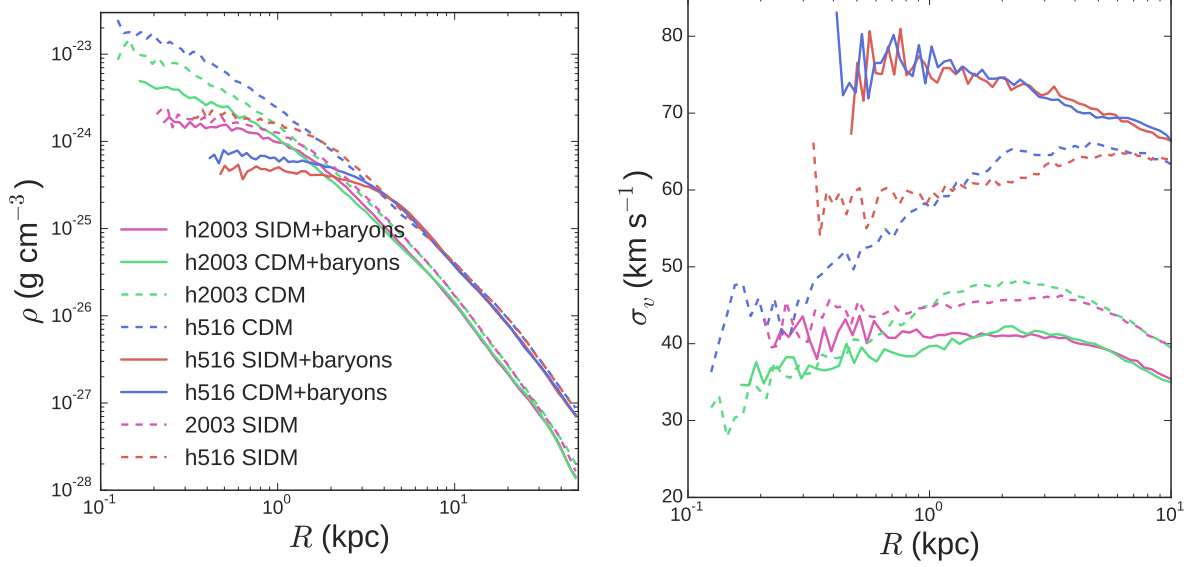


Figure 3. RADIAL PROFILES. Left: The radial density profile of the DM component for halos/galaxies h516 and h2003. Right: The velocity dispersion of DM component in the same halos/galaxies. h516-CDM: blue. h516-SIDM: red. h2003-CDM: cyan. h2003-SIDM: magenta. Dashed: DM-only runs. Both density and dispersion profiles become similar in CDM vs SIDM once baryonic processes are introduced.

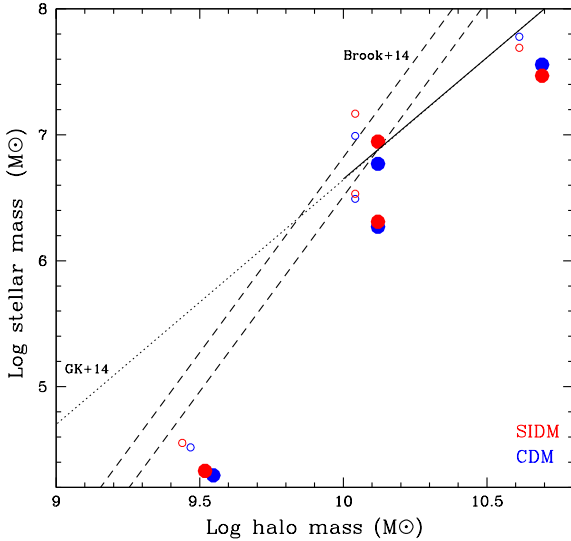


Figure 4. STELLAR MASS/HALO MASS RELATION: The Stellar Mass - Halo Mass relation for the simulated galaxies. Dashed lines and solid lines show the relation obtained from Local Group data (Brook & Di Cintio 2014; Garrison-Kimmel et al. 2014). The relations are extrapolated below $\sim 10^{6.5} M_{\odot}$ due to sample incompleteness (dotted lines). Circles show the raw data, solid dots show the simulation data correcting for observational and simulation biases (Munshi et al. 2013) in measuring stellar and halo masses. Overall the simulations produce the right amount of stars. The most massive halo converts about 1% of gas into stars. The rapid drop in SF efficiency at halo masses below $10^{10} M_{\odot}$ is due to the introduction of ‘early feedback’ (see text).

rapidly. A factor of two in the DM content within 100-500 pc of faint field dwarfs, could be revealed by large spectroscopic samples of the associated stellar populations (M. Walker, private communication). We also verified that at larger V_{max} the density profiles of

the DM-only halos match those recently published in (Elbert et al. 2014), which at $V_{max} \sim 35 \text{ km s}^{-1}$ form significant cores (see also next section where the effect of baryons in these larger systems is included). This result confirms our simple analytical expectations and shows that even with a significant constant SIDM cross section, DM cores rapidly become smaller than our resolved scale ($\sim 100\text{-}200 \text{ pc}$ or twice the spline kernel softening) in field halos with virial mass $< 10^{10} M_{\odot}$ and $V_{max} < 30 \text{ km s}^{-1}$. Confirming the results from Li et al. (2008) and extending them to much smaller halo masses and higher resolution we verified that the increased τ_{SI} at small halo masses comes not only from a lower σ_{DM} but also from lower cusp densities, possibly due to the later epoch of collapse of the central regions of a halo. We verified the DM density within the central 250 pc decreases by a factor of eight in CDM halos with mass from $10^8 M_{\odot}$ compared to halos of $10^{10} M_{\odot}$. If we look at the average densities as a function of V_{max} , another difference emerges between the SIDM field (circled red crosses) and satellites (red crosses), with satellite halos showing central densities lower by about factor of two compared to field halos of similar V_{max} . This important environmental difference could be due to the satellites forming their central regions earlier, or to the significant boost to ρ and v_{max} in eq.3 due to their orbiting 1) inside the dense halo of a much more massive host and 2) at a much higher speed than their internal velocity dispersion. Our simulations were able to highlight this difference as our simulations resolve field *and* satellites halos with significantly lower peak velocities ($10\text{-}20 \text{ km s}^{-1}$) than in previous works.

The main result from this section is that evidence of DM cores in real galaxies with $V_{max} < 30 \text{ km s}^{-1}$ would constrain the SIDM cross section to values $\sigma \gg 2 \text{ cm}^2/\text{g}$ when the typical DM velocity dispersion is low. If significant DM cores are found in these galaxies, their existence would give support to models with a variable SIDM cross section that is higher ($20 \text{ cm}^2/\text{g}$, see eq.2) at small halo masses and then declines rapidly at the scale of groups and galaxy clusters as constraints at scale support small cross sections $\sigma < 1 \text{ cm}^2/\text{g}$. We plan to further explore the relative effect of stronger

Run ID	Halo Mass CDM/SIDM	V_{max} km s ⁻¹	Stellar Mass CDM/SIDM	HI mass CDM/SIDM
h516	4.1×10^{10}	58.4	$6.2/4.9 \times 10^7$	$3.3/2.0 \times 10^8 M_\odot$
h516b	1.1×10^{10}	33.0	$9.8/14.7 \times 10^6$	$1.6/0.94 \times 10^8 M_\odot$
h2003	1.1×10^{10}	30.5	$3.1/3.4 \times 10^6$	$5.0/16.6 \times 10^6 M_\odot$

Table 2. THE TOTAL HALO MASS, STELLAR AND HI MASSES AND V_{max} (IN KM S⁻¹) FOR SOME REPRESENTATIVE HALOS IN THE CDM RUNS WITH SF AND THEIR SIDM COUNTERPARTS. $z=0$ STELLAR MASSES WERE MEASURED WITHIN 2.5KPC. h516b IS THE SECOND MOST MASSIVE HALO IN THE h516 RUN.

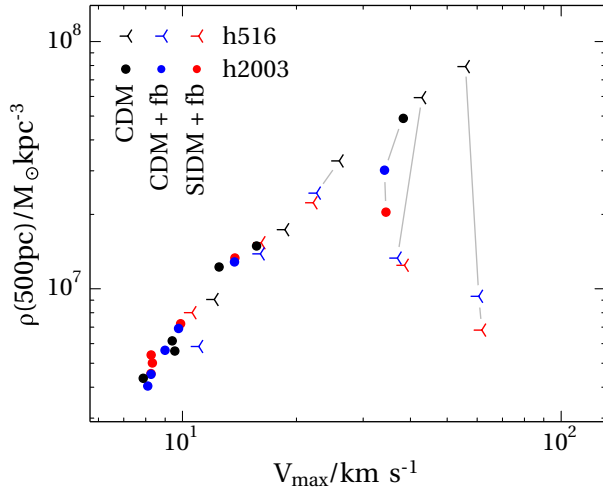


Figure 5. EFFECTS OF BARYONS PHYSICS: The central density of CDM-only halos (blue) vs their SIDM (red) counterparts run with baryon physics and bursty feedback. Lines connect the DM-only runs of h516 and h2003 to their counterparts with baryons. For our choice of the SIDM interaction cross section and for halos with $V_{max} > 50$ km s⁻¹ (corresponding to stellar masses larger than $10^8 M_\odot$) the central mass of CDM and SIDM halos is similar, but significantly lower than the predictions of CDM-only runs. Due to low DM interaction rates and lack of bursty outflows, at lower halo masses both cosmologies give similar predictions: cuspy central DM profiles. Larger SIDM cross sections would be able to differentiate the various models in halos with $V_{max} < 20$ km s⁻¹ as DM cores would then form in galaxies where baryon physics do not play a major role.

SIDM interactions on satellites compared to field halos in future work.

3.2 Simulations with SF: SIDM similar to CDM when Baryon Physics are relevant.

We focused our hydrodynamical simulations on the largest galaxies formed in the filamentary regions ‘h516’ and ‘h2003’. These are two well studied fields: h2003 is the same halo simulated in Governato et al. (2015) while h516 is the main halo of Governato et al. (2010) and of the “7 dwarfs” galaxies sample studied in Shen et al. (2014) and Madau et al. (2014). The SF parameters in our study were identical for all CDM and SIDM simulations. They also correspond to the fiducial “g5” runs in Governato et al. (2015), where we explored the effects of different feedback and SF recipes in the context of comparing the formation of dwarfs in CDM vs Warm scenarios. Here we emphasize that our SF implementation creates repeated starbursts and gas outflows with significant loading factors (gas mass ejected from the center divided by star formation rate).

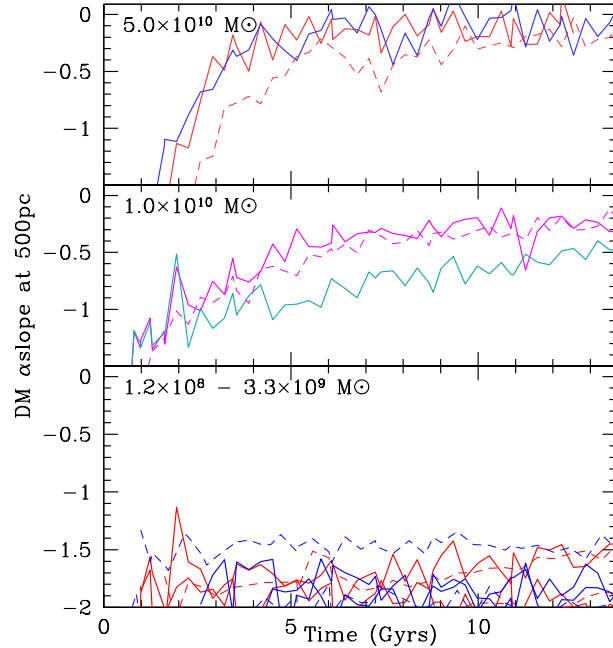


Figure 6. THE SLOPE α OF THE DM DENSITY PROFILE IN SIDM AND CDM OVER DIFFERENT MASS RANGES: blue and cyan: CDM, red and magenta: SIDM, solid lines: baryon+DM runs, dashed lines: DM-only runs. Top: halo h516. The DM slope evolves rapidly and in a similar way in both CDM and SIDM, as dynamical heating is very efficient at this scale. Middle: halo h2003. (blue: CDM, red: SIDM). Bottom: a collection of field halos with total mass $< 10^9 M_\odot$ from our simulations. SF efficiency is too low and the SIDM interaction rate is too low to create cores.

Multi-wavelength evidence for outflows, analysis of the stellar populations in the SDSS dwarfs and realistic CMDs (Governato et al. 2015) give strong support to our implementation of SF. This approach differs from the SIDM study of Vogelsberger et al. (2014) where less bursty feedback still removes gas from galaxy centers, but does not create substantial DM cores. The baryonic content of the galaxies in our study are summarized in Table 2.

Figure 3 (left panel) compares the density profiles of the DM component of galaxies h516 and h2003. In DM-only simulations halos with masses $> 10^{10} M_\odot$ have cuspy profiles (halo h2003: cyan dashed, halo h516: blue dotted). Once baryon physics and outflows are introduced, flatter DM profiles are created in both SIDM and CDM cosmologies. The blue dashed (CDM-only) vs blue (CDM+SF) lines and the red (SIDM+SF) show results for h516. The cyan dashed (CDM-only) vs cyan solid (CDM+SF) lines and the magenta (SIDM+SF) lines show results for h2003, the smaller halo. In both CDM and SIDM models the central cuspy profiles have been significantly flattened inside 1 kpc. h516, the most massive halo studied with the inclusion of SF, is the one where the central DM density decreases the most. This result is consistent with previous findings (Governato et al. 2012; Di Cintio et al. 2014), showing that the efficiency of core formation peaks in halos with $V_{max} \sim 50$ km s⁻¹.

Figure 3 (right panel) compares instead the velocity dispersion profiles of the DM component in halos h516 and h2003. As for the density profiles, DM-only runs of different cosmologies have different local DM velocity distribution profiles: CDM halos show a decreasing dispersion closer the halo center while the SIDM halos show a rather flat profile. This difference, a result of the energy transfer to the center of the halo due to collisional processes, had

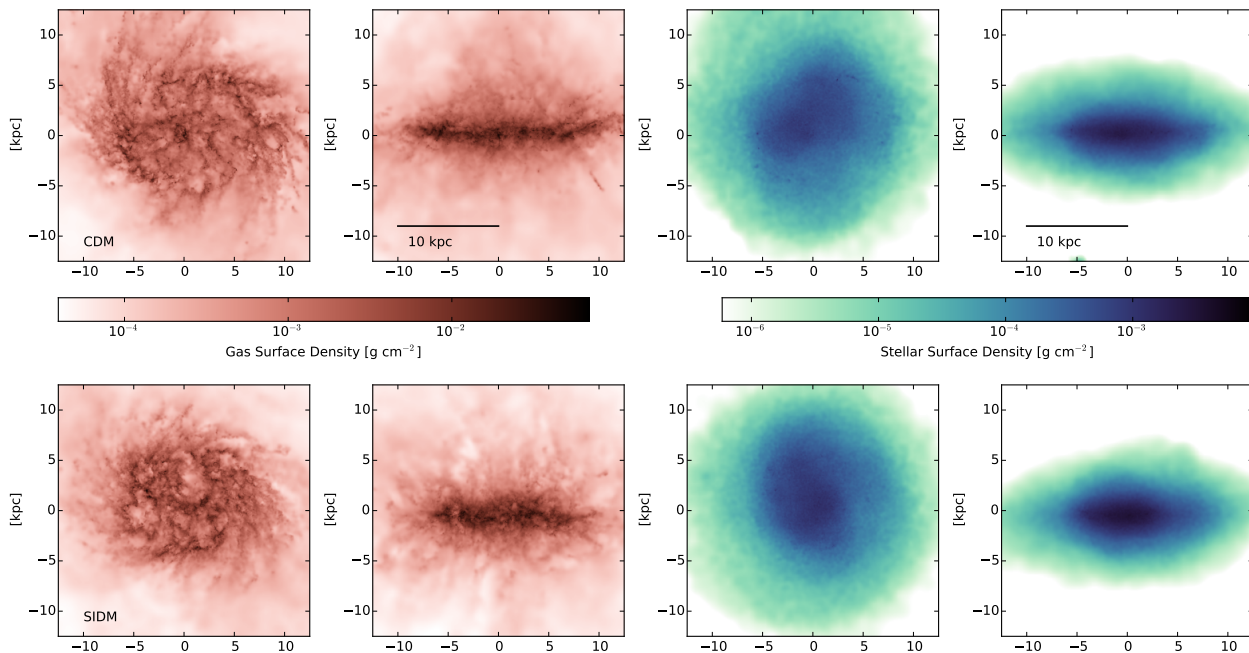


Figure 7. THE PROJECTED COLOR DENSITY MAP OF THE BARYON DISTRIBUTION IN GALAXY H516. Top: CDM. Bottom: SIDM. Left panels: projected gas density at $z=0$ seen edge-on and face-on. Right panels: Stellar projected density at $z=0$. The stellar disks are relatively thicker than in earlier simulations (Governato et al. 2010), an effect of the introduction of ‘early feedback’ from young stars. We verified that in both models the stellar distribution is exponential, with a similar disc scale length and lack of a central dense spheroid.

been considered a strong signature of SIDM. However this difference is erased by the introduction of bursty feedback, that creates significant DM cores in the CDM halos. ‘Dynamical heating’ also causes the velocity dispersion profiles of all halos to flatten out.

Figure 4 shows the stellar mass/halo mass ratio of the halos we simulated with the inclusion of baryon physics, showing that they follow the stellar mass/halo mass relation inferred using local data and the abundance matching technique (Brook & Di Cintio 2014; Garrison-Kimmel et al. 2014). This is particularly relevant as producing the correct amount stars is necessary to estimate the minimum mass at which baryonic processes can originate cores. After this paper was submitted (Oñorbe et al. 2015) published results from a simulated CDM halo of similar total mass, which also formed about $10^6 M_\odot$ in stars, leading to a cored DM profile.

Figure 5 shows the DM central densities as a function of halo peak velocity once SF is included. The comparison with Figure 1 is striking: where at $V_{max} > 30 \text{ km s}^{-1}$ CDM was clearly differentiated from SIDM, now the central density of CDM and SIDM halos is almost identical over the whole 10 to 50 km s^{-1} range. This result clearly illustrates how predictions from DM-only runs can be completely superseded by the addition of the complex baryon – DM interactions.

In Figure 6 we investigate how the slope of the DM profile (measured at 500 pc) evolves with time in a sample of field halos with a range of masses. As the mechanisms of core formation differ (potential fluctuations linked to SF vs SIDM collisions) the time evolution of the DM slope may also be significantly different. We have found that the evolution of the systems can be roughly divided in three stellar mass ranges. Present day systems with stellar masses larger than $10^8 M_\odot$ ($V_{max} > 50 \text{ km s}^{-1}$ as in classic field dwarfs) had cored DM profiles since redshift > 4 , with no significant differ-

ence between SIDM and CDM (top panel). In the SIDM-only run, the DM core forms more slowly than when the effect of baryons are included. The effect of baryon feedback on the DM profile is clearly detectable as soon as about $10^6 M_\odot$ of stars have been created (see also Governato et al. 2015; Peñarrubia et al. 2012). In galaxies with present day stellar masses below $10^{7-8} M_\odot$, the effect of ‘dynamical heating’ induced by feedback is progressively reduced (Governato et al. 2012, 2015; Di Cintio et al. 2014). At the radial scale of 500 pc the CDM and SIDM halos of h2003 show DM profiles that start cuspy and then slowly develop a flatter profile. In both SIDM and CDM the process is more gradual compared to more massive systems, due to a number of factors (star formation rates are lower and τ_{SI} is longer). However, the inclusion of baryonic processes again makes the galaxy evolve similarly in CDM vs SIDM. By redshift $z < 1$ the difference in DM slopes is not significant enough to discriminate between SIDM and CDM. Halo h2003 was also recently run in a WDM cosmology (Governato et al. 2015). Similar to the CDM case the WDM cusp turned into a core over time, due to bursty feedback. By $z=0$ the central DM distribution of halo h2003 is similar in CDM, WDM (Governato et al. 2015) and SIDM (this work).

At even smaller masses, the evolution of the DM slope α with the inclusion of baryonic processes (continuous lines) confirms the results from the DM-only runs (dashed lines). SF at such small scales is strongly inhibited by the cosmic UV field. Similarly, at such small masses the SIDM interaction timescale becomes long compared to the Hubble time and the survival time of the halo. Hence the central DM slope measured at 500pc is not significantly different in SIDM vs CDM halos, as predicted by the empirical calculations in the previous section. The failure of SIDM to form substantial DM cores in very faint dwarfs with host halos with mass

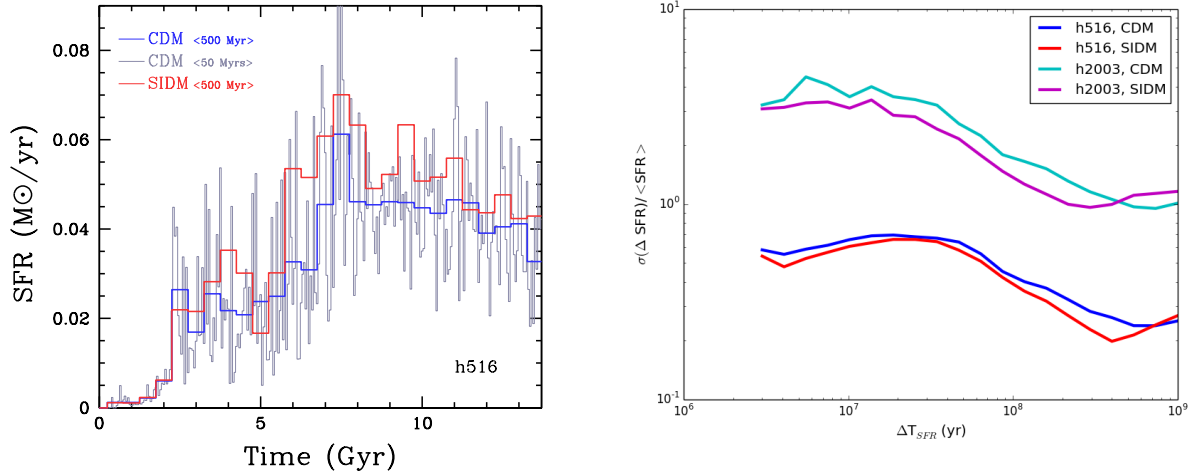


Figure 8. THE SFR AS A FUNCTION OF COSMIC TIME. Left panel: halo h516 in CDM and SIDM cosmologies. Both galaxies have extended, gas rich disks and negligible bulges. Right panel: the burstiness of models h516 and h2003 in CDM and SIDM, measured at different timescales (see text for a definition). SF does not differ significantly in CDM vs SIDM, and appears to be mostly regulated by feedback and accretion rates.

$< 10^{10} M_{\odot}$ had not been explored in previous numerical works, where high resolution simulations mostly focused on halos more massive than $10^{10} M_{\odot}$.

Overall, the inclusion of SF and baryonic processes erase the differences seen in the DM-only runs. At the scale of dwarf galaxies with $V_{\text{peak}} \sim 30\text{--}50 \text{ km s}^{-1}$, energy transfer to the DM makes the DM distribution at the center of galaxies flatter than an NFW profile and almost identical in CDM vs SIDM. As a result current constraints on the SIDM cross section from dwarf sized field come out considerably weakened and will have to be reconsidered. Moreover, we predict (see Figure 1) that a SIDM cross section $> 10 \text{ cm}^2/\text{g}$ would be necessary to create DM cores in smaller halos with $V_{\text{max}} < 10 \text{ km s}^{-1}$. As the shapes of galaxy clusters require a SIDM cross section smaller than $1 \text{ cm}^2/\text{g}$ (Peter et al. 2013). If cores exist in dwarf galaxies, these results argue in favor of a variable SIDM cross section (see also Vogelsberger et al. (2012)).

3.3 Star Formation Histories and Assembly of the baryonic component

In this section we analyze the $z = 0$ baryonic distribution of the galaxies that form stars in our simulations, while focusing on the two main halos: h2003 and h516. We verified that in both CDM and SIDM cosmologies the stellar mass of galaxy h516 follows an exponential profile with no spheroidal component. The projected gas and stellar densities of galaxy h516 are shown in Figure 7, showing a similar distribution in CDM vs SIDM. Both stellar discs are thick and dynamically hot (Figure 7) and more extended than the CDM version of h516 described in Christensen et al. (2014a), an effect of the introduction of early feedback (Trujillo-Gomez et al. 2013; Roškar et al. 2014). Confirming the visual impression from Figure 7, we verified that the radial distribution of stars at $z=0$ does not change significantly in the CDM galaxies vs their SIDM counterparts, both following a trend for larger systems to have more

extended stellar systems and roughly consistent with observational data. The half light radius for h516b (Table 1) is for example, 2.0 kpc in SIDM, vs 1.8 kpc in CDM. This is a different outcome compared to the results of a less bursty SF scenario as the one studied in Vogelsberger et al. (2014), which followed galaxies in a similar mass range to ours. In their simulations the SIDM distribution is less concentrated compared to the CDM one, leading “to dwarf galaxies with larger stellar cores and smaller stellar central densities.” In our simulations the dynamical coupling of baryons to DM, driven by fast and repeated outflows, shapes the stellar distribution and leads to a similar baryon distribution and content.

Furthermore, with the adopted SF prescription, the star formation histories (SFH) of the galaxies formed in the CDM model look very similar to the SIDM counterparts. This is most likely due to two main reasons: 1) the assembly rate of both DM and baryons, being driven by the large scale structure remains unchanged in SIDM and 2) there is no difference in the central DM distribution between the two models as it responds quickly to the effects of feedback. As an example, Figure 8 shows the SFH of halo h516 in the CDM and SIDM models, which show a very similar time evolution, peaking 5 Gyrs after the Big Bang. Overall, SIDM and CDM halos have almost identical DM masses by $z=0$ and the SF efficiency is similar, within 20% in the two models. This result differs from the CDM vs WDM comparison in Governato et al. (2015), where the WDM version of h2003 formed only half the stars due to the delayed assembly of the halo (see also Colín et al. 2015). However, changes on the timescale and intensity of the individual SF events could be driven by subtle effects and still differentiate between CDM and SIDM, for example a shallower density profile could drive more gas instabilities that lead to radial inflows and increase the burstiness of SF, or, on the other hand, lower DM densities could slow down the collapse of gas and reduce SF in the SIDM scenario. We quantified the burstiness of SF in SIDM vs CDM by measuring the dispersion in star formation rates (SFR) measured

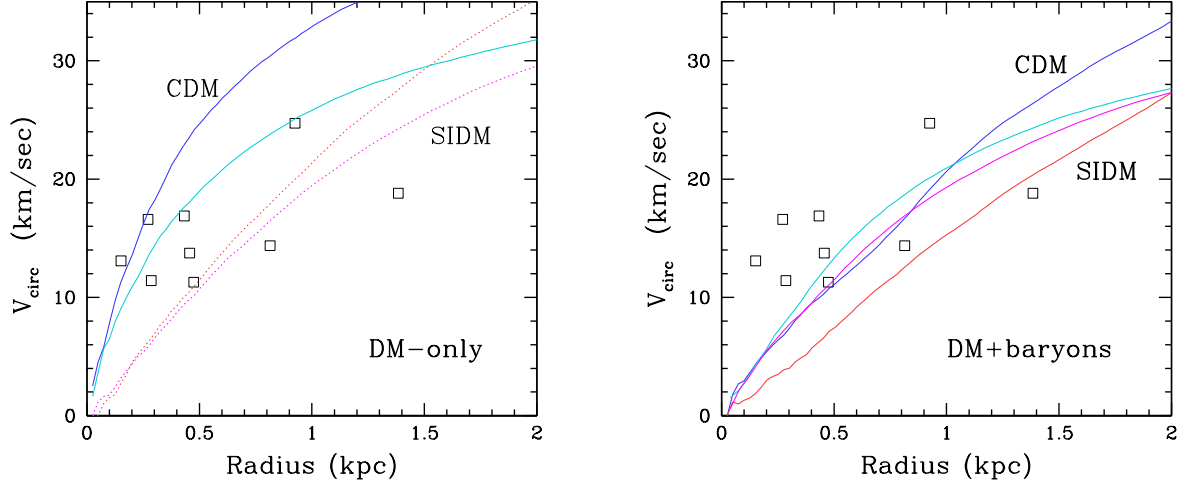


Figure 9. THE ROTATION CURVES V_c of halos h516 and h2003 in CDM (blue and cyan) and SIDM (red and magenta) compared with the observational constraints from a sample of Local Group field dwarfs (Wolf et al. 2010; McConnachie 2012; Weisz et al. 2014). The introduction of feedback processes lowers V_c out to at least 2 kpc, where mass decomposition based on HI kinematics are crucial. (V_c is defined as $= (GM/r)^{1/2}$). Softening is 64pc for h2003 and 86pc for h516.

in ΔT_{SFR} intervals, where ΔT_{SFR} was varied from 10^6 to 10^9 years (for a similar approach but different definition of burstiness, see Hopkins et al. 2014). Measuring ΔT_{SFR} over hundreds of randomly sampled intervals, bursty SF at a given time scale shows as a large dispersion if the SF rate at a time $T + \Delta T_{SFR}$ differs substantially from the SFR at a previous time T . The right panel of Figure 8 shows that the burstiness measured over different timescales was similar for both halo h516 and h2003 in both models. Both h516 and h2003 show a SF rate dominated by small time scale fluctuations, with a similar dependence on time scale and halo mass, with the less massive halos having a burstier SF at all time scales (a result seen also in simulations with different feedback models, e.g., Hopkins et al. 2014). Observations of nearby stellar populations and comparisons with simulations (Tolstoy et al. 2009; Kauffmann 2014; Governato et al. 2015; Weisz et al. 2014) strongly support a bursty build up of the stellar content of dwarf galaxies. We verified that our set of simulations qualitatively reproduce the fraction of stars formed in bursts as estimated in Kauffmann (2014): 20-50% with a larger fraction formed in the less massive system. Bursts were defined as periods with $SF > 2 - 4 \times \langle SFH \rangle$ and duration of 10^7 - 10^8 years. A burstier implementation of our SF model (as one that neglected HI self shielding) would be ruled out by excessive structure in the stellar CMD, as discussed in Governato et al. (2015).

Overall, Within our small sample of galaxies, we do not find evidence of large differences in the baryonic content and distribution in galaxies formed in a CDM vs SIDM model.

Finally, Figure 9 show the rotation curves V_c (defined as $\sqrt{GM(<r)/r}$) of our galaxies h516 and h2003 compared to estimates from a sample of local dwarfs (empty squares, from Wolf et al. 2010; Weisz et al. 2014). The left panel shows the well known result that halos formed in CDM-only simulations have higher central mass densities that most observed dwarfs (although significant

uncertainties remain on the observational estimates). At the same time, SIDM-only runs with a range of cross sections (Elbert et al. 2014) show a better agreement with observational estimates as the central DM densities are lower. However, the right panel of Figure 7 shows that once baryon physics are introduced, the central mass distribution (DM+baryons) of CDM dwarfs matches the observational data, equally well, without requiring SIDM. Recent works have compared dwarf galaxies in the Local Group (Brook & Di Cintio 2014; Sawala et al. 2015) and MW satellites Zolotov et al. (2012); Arraki et al. (2014) with simulations. They have shown how the introduction of feedback (and tidal processes for satellites) generates a realistic $M_{star} - M_{halo}$ relation, as galaxies at a fixed M_{star} are hosted by more massive halos than when a universal NFW profile is assumed in the analysis³. This result shows how the perceived discrepancy between the observed number density of field galaxies as a function of V_{max} and that of the underlying halo population is naturally accounted for in a CDM context where feedback is introduced and the central total density is lowered. In good agreement with results from our simulations, the revised abundance matching from Brook & Di Cintio (2014) predict that field galaxies are hosted in halos with mass $> 5 \times 10^9 M_\odot$, with most halos below that threshold being devoid of stars. Our results provide direct evidence that SIDM-only simulations mimic the effects of feedback, but also that *when bursty feedback is introduced, SIDM galaxies are essentially indistinguishable from their CDM counterparts*. Both SIDM and CDM models create galaxies with mass distributions and observable properties in broad agreement with the observed ones.

³ in a halo model with a central mass density lower than NFW the V_{circ} measured at ~ 1 kpc translates to the same V_{peak} and hence halo mass of an NFW halo. As a consequence, an observed V_{circ} translates to higher halo host mass than when a more concentrated NFW halo is assumed.

4 CONCLUSIONS

We studied a set of cosmological simulations of field dwarf galaxies in CDM and SIDM. The SIDM simulations include for the first time a description of bursty SF and feedback that creates potential fluctuations able to lower the central DM density of halos where at least $10^6 M_\odot$ of stars have formed. The force resolution of our simulations (64-86 pc with a spline kernel softening) allows us to resolve with many thousands of particles the central regions of halos (and millions to the virial radius) down to halo masses where the impact of star formation will not play a major role and where the effect of SIDM alone dominates. A relatively large value ($2 \text{ cm}^2/\text{g}$ for the SIDM cross section) was chosen to maximize its difference from the CDM model. We have also run a set of DM-only simulations that allowed us to study the evolution of a uniform resolution set of DM halos down to masses of only few times $10^8 M_\odot$ (equivalent to $V_{\text{max}} < 20 \text{ km s}^{-1}$) both in the field and in the dense environment of a more massive host. Our results can be summarized by three main findings:

- Once SF and resulting feedback is introduced, the central DM mass distribution and velocity dispersion becomes similar for CDM and SIDM galaxies with stellar masses in the 10^6 – $10^8 M_\odot$ range and circular velocity 25-50 km/sec (Fig.3). At the scale of 0.5–2 kpc the total matter content is in good agreement with observational estimates of Local Group dwarfs. This result differs starkly from the predictions of DM-only simulations, or simulations where energy feedback does not lead to core formation (Boylan-Kolchin et al. 2011; Garrison-Kimmel et al. 2014).

- Analytical expectations and simulations show that with a fixed SIDM cross section of $2 \text{ cm}^2/\text{g}$ the DM central density and internal velocities of halos with mass below $10^9 M_\odot$ are too low to have a significant number of DM–DM interactions. Such SIDM halos remain cuspy when observed at a scale of 500pc, and show an enclosed DM mass content lower by about only a factor 2 compared to their CDM counterparts (Fig.1 & 2). This result poses an interesting *lower limit* to the SIDM cross section in halos associated with galaxies with stellar masses below $10^6 M_\odot$. If kpc sized DM cores are found in these galaxies, their existence would give support to models with a variable SIDM cross section that is high (~ 10 – $20 \text{ cm}^2/\text{g}$, see eq.2) at small halo masses and then declines rapidly at the scale of galaxies and clusters. Large cross sections at dwarf scales are also suggested by DM-only studies (Elbert et al. 2014). Such large cross sections may have a detectable effect on the SFHs of dwarf sized systems, but could also make galaxy satellites easier to disrupt. Our simulations also highlight the relative environmental effects of the enhanced interaction rate at the center of very small satellites compared to their field counterparts, due to rapid orbital velocities in the dense halos of a massive host. This relative difference offers the potential of using faint galaxies to constrain the cross section of SIDM as a function of the DM velocity.

- Once regulated by feedback, the SFHs (Fig.7), stellar and gas content and spatial distribution do not differ substantially in CDM vs SIDM model, both forming gas rich galaxies with bulgeless disks which resemble real ones.

These results lead to potentially important implications for SIDM models. As baryons lead to a drastic change in the mass distribution of central regions of typical dwarf galaxies with $V_c \sim 30$ – 60 km/sec , many of the current bounds on the SIDM cross section at different mass scales will need to be re-examined. After the introduction of realistic descriptions of SF and feedback. Both CDM and SIDM form dwarf galaxies with DM distribution and

observable properties in broad agreement with observational data. As a result, while certainly not excluded, SIDM is not necessary to solve the problem of the excess of DM at the center of simulated dwarf galaxies with $V_{\text{max}} > 30 \text{ km s}^{-1}$. Furthermore, because the effect of SIDM becomes negligible at very small galaxy/halo masses even with a relatively large constant velocity cross section ($2 \text{ cm}^2/\text{g}$), SIDM with a velocity dependent cross section will become necessary if even very faint dwarf galaxies are observed to have dark matter cores. This work highlights how simulations that a) include realistic SF and feedback processes and b) study a large sample of faint dwarfs are necessary to take advantage of astrophysical constraints on DM models.

ACKNOWLEDGMENTS

ABF was funded by Washington NASA Space Grant Consortium, NASA Grant NNX10AK64H. FG and TQ were funded by NSF grant AST-0908499. FG acknowledges support from NSF grant AST-0607819 and NASA ATP NNX08AG84G. AP is supported by a Royal Society University Research Fellowship. Some results were obtained using the analysis software pynbody, (Pontzen et al. 2013). ChaNGa was developed with support from National Science Foundation ITR grant PHY-0205413 to the University of Washington, and NSF ITR grant NSF-0205611 to the University of Illinois. We thank Haibo Yu, Sean Tulin, Matt Walker and Lucio Mayer for stimulating discussions and a careful reading of the manuscript. We thank the referee for constructive comments.

REFERENCES

- Adams J. J. et al., 2014, ApJ, 789, 63
- Agertz O., Kravtsov A. V., 2014, ArXiv 1404.2613
- Arraki K. S., Klypin A., More S., Trujillo-Gomez S., 2014, MNRAS, 438, 1466
- Avila-Reese V., Colín P., Gottlöber S., Firmani C., Maulbetsch C., 2005, ApJ, 634, 51
- Binney J., Gerhard O., Silk J., 2001, MNRAS, 321, 471
- Boylan-Kolchin M., Bullock J. S., Kaplinghat M., 2011, MNRAS, 415, L40
- Brook C. B., Di Cintio A., 2014, ArXiv 1410.3825
- Brook C. B. et al., 2011, MNRAS, 415, 1051
- Brook C. B., Stinson G., Gibson B. K., Wadsley J., Quinn T., 2012, MNRAS, 424, 1275
- Brooks A. M., 2014, AdPhysik 10.1002/andp.201400068, 10
- Brooks A. M., Zolotov A., 2014, ApJ, 786, 87
- Buckley M. R., Zavala J., Cyr-Racine F.-Y., Sigurdson K., Vogelsberger M., 2014, Phys. Rev. D, 90, 043524
- Burkert A., 2000, ApJ, 534, L143
- Christensen C. R., Brooks A. M., Fisher D. B., Governato F., McCleary J., Quinn T. R., Shen S., Wadsley J., 2014a, MNRAS, 440, L51
- Christensen C. R., Governato F., Quinn T., Brooks A. M., Shen S., McCleary J., Fisher D. B., Wadsley J., 2014b, MNRAS, 440, 2843
- Colín P., Avila-Reese V., González-Samaniego A., Velázquez H., 2015, ApJ, 803, 28
- Colín P., Avila-Reese V., Valenzuela O., Firmani C., 2002, ApJ, 581, 777
- Cyr-Racine F.-Y., Sigurdson K., 2013, Phys. Rev. D, 87, 103515

- Davé R., Spergel D. N., Steinhardt P. J., Wandelt B. D., 2001, *ApJ*, 547, 574
- Del Popolo A., 2009, *ApJ*, 698, 2093
- Di Cintio A., Brook C. B., Macciò A. V., Stinson G. S., Knebe A., Dutton A. A., Wadsley J., 2014, *MNRAS*, 437, 415
- Domínguez A., Siana B., Brooks A. M., Christensen C. R., Bruzual G., Stark D. P., Alavi A., 2014, *arXiv:1408.5788*
- D’Onghia E., Burkert A., 2003, *ApJ*, 586, 12
- Elbert O. D., Bullock J. S., Garrison-Kimmel S., Rocha M., Oñorbe J., Peter A. H. G., 2014, *arXiv:1412.1477*
- Feng J. L., Kaplinghat M., Tu H., Yu H.-B., 2009, *J. Cosmol. Astropart. Phys.*, 7, 4
- Feng J. L., Kaplinghat M., Yu H.-B., 2010, *Physical Review Letters*, 104, 151301
- Garrison-Kimmel S., Boylan-Kolchin M., Bullock J. S., Kirby E. N., 2014, *ArXiv 1404.5313*
- Geach J. E., 2015, *Nature*, 519, 423
- Gnedin O. Y., Ostriker J. P., 2001, *ApJ*, 561, 61
- Governato F. et al., 2010, *Nature*, 463, 203
- Governato F. et al., 2015, *MNRAS*, 448, 792
- Governato F. et al., 2012, *MNRAS*, 422, 1231
- Hernquist L., 1990, *ApJ*, 356, 359
- Hopkins P. F., Kereš D., Oñorbe J., Faucher-Giguère C.-A., Quataert E., Murray N., Bullock J. S., 2014, *MNRAS*, 445, 581
- Jetley P., Gioachin F., Mendes C., Kale L. V., Quinn T. R., 2008, in *Proceedings of IEEE International Parallel and Distributed Processing Symposium 2008*
- Kahlhoefer F., Schmidt-Hoberg K., Frandsen M. T., Sarkar S., 2014, *MNRAS*, 437, 2865
- Kaplinghat M., Keeley R. E., Linden T., Yu H.-B., 2014, *Physical Review Letters*, 113, 021302
- Katz N., White S. D. M., 1993, *ApJ*, 412, 455
- Kauffmann G., 2014, *MNRAS*, 441, 2717
- Kim J.-h. et al., 2014, *ApJS*, 210, 14
- Klypin A., Kravtsov A. V., Valenzuela O., Prada F., 1999, *ApJ*, 522, 82
- Koda J., Shapiro P. R., 2011, *MNRAS*, 415, 1125
- Kroupa P., 2001, *MNRAS*, 322, 231
- Li Y., Mo H. J., Gao L., 2008, *MNRAS*, 389, 1419
- Loeb A., Weiner N., 2011, *Physical Review Letters*, 106, 171302
- Lundgren B. F. et al., 2012, *ApJ*, 760, 49
- Madau P., Shen S., Governato F., 2014, *ApJ*, 789, L17
- Martin C. L., Shapley A. E., Coil A. L., Kornei K. A., Bundy K., Weiner B. J., Noeske K. G., Schiminovich D., 2012, *ApJ*, 760, 127
- Martinez G. D., Bullock J. S., Kaplinghat M., Strigari L. E., Trotta R., 2009, *JCAP*, 6, 14
- Mashchenko S., Wadsley J., Couchman H. M. P., 2008, *Science*, 319, 174
- McConnachie A. W., 2012, *AJ*, 144, 4
- Menon H., Wesolowski L., Zheng G., Jetley P., Kale L., Quinn T., Governato F., 2014, *ArXiv 1409.1929*
- Moore B., Gelato S., Jenkins A., Pearce F. R., Quilis V., 2000, *ApJ*, 535, L21
- Moore B., Ghigna S., Governato F., Lake G., Quinn T., Stadel J., Tozzi P., 1999a, *ApJ*, 524, L19
- Moore B., Quinn T., Governato F., Stadel J., Lake G., 1999b, *MNRAS*, 310, 1147
- Munshi F. et al., 2013, *ApJ*, 766, 56
- Navarro J. F., Frenk C. S., White S. D. M., 1996, *ApJ*, 462, 563
- Newman A. B., Treu T., Ellis R. S., Sand D. J., Nipoti C., Richard J., Jullo E., 2013, *ApJ*, 765, 24
- Oñorbe J., Boylan-Kolchin M., Bullock J. S., Hopkins P. F., Kerš D., Faucher-Giguère C.-A., Quataert E., Murray N., 2015, *ArXiv e-prints*
- Oh S., de Blok W. J. G., Walter F., Brinks E., Kennicutt R. C., 2008, *AJ*, 136, 2761
- Oh S.-H., de Blok W. J. G., Brinks E., Walter F., Kennicutt, Jr. R. C., 2011, *AJ*, 141, 193
- Papastergis E., Giovanelli R., Haynes M. P., Shankar F., 2015, *A&A*, 574, A113
- Peñarrubia J., Pontzen A., Walker M. G., Koposov S. E., 2012, *ApJ*, 759, L42
- Peter A. H. G., Rocha M., Bullock J. S., Kaplinghat M., 2013, *MNRAS*, 430, 105
- Pontzen A., Governato F., 2012, *MNRAS*, 421, 3464
- Pontzen A., Governato F., 2014, *Nature*, 506, 171
- Pontzen A., Roskar R., Stinson G., Woods R., 2013, *pynbody: N-Body/SPH analysis for python. Astrophysics Source Code Library*
- Power C., Navarro J. F., Jenkins A., Frenk C. S., White S. D. M., Springel V., Stadel J., Quinn T., 2003, *MNRAS*, 338, 14
- Quinn T. R., Jetley P., Kale L. V., Gioachin F., 2013, in *Parallel Science and Engineering Applications: The Charm++ Approach*, Kale L. V., Abhinav B., eds., Taylor & Francis Group, CRC Press
- Ritchie B. W., Thomas P. A., 2001, *MNRAS*, 323, 743
- Rocha M., Peter A. H. G., Bullock J. S., Kaplinghat M., Garrison-Kimmel S., Oñorbe J., Moustakas L. A., 2013, *MNRAS*, 430, 81
- Roškar R., Teyssier R., Agertz O., Wetzstein M., Moore B., 2014, *MNRAS*, 444, 2837
- Sawala T. et al., 2015, *MNRAS*, 448, 2941
- Schutz K., Slatyer T. R., 2015, *J. Cosmol. Astropart. Phys.*, 1, 21
- Shen S., Madau P., Conroy C., Governato F., Mayer L., 2014, *ApJ*, 792, 99
- Shen S., Wadsley J., Stinson G., 2010, *MNRAS*, 407, 1581
- Spergel D. N., Steinhardt P. J., 2000, *Physical Review Letters*, 84, 3760
- Stinson G., Brook C., Macciò A. V., Wadsley J., Quinn T. R., Couchman H. M. P., 2012, *ArXiv 1208.0002*
- Stinson G., Seth A., Katz N., Wadsley J., Governato F., Quinn T., 2006, *MNRAS*, 373, 1074
- Strigari L. E., Kaplinghat M., Bullock J. S., 2007, *PRD*, 75, 061303
- Teyssier R., Pontzen A., Dubois Y., Read J. I., 2013, *MNRAS*, 429, 3068
- Tolstoy E., Hill V., Tosi M., 2009, *ARAA*, 47, 371
- Trujillo-Gomez S., Klypin A., Colin P., Ceverino D., Arraki K., Primack J., 2013, *ArXiv 1311.2910*
- Tulin S., Yu H.-B., Zurek K. M., 2013, *PRD*, 87, 115007
- van den Bosch F. C., Burkert A., Swaters R. A., 2001, *MNRAS*, 326, 1205
- van der Wel A. et al., 2011, *ApJ*, 742, 111
- Velliscig M., van Daalen M. P., Schaye J., McCarthy I. G., Cacciato M., Le Brun A. M. C., Dalla Vecchia C., 2014, *arXiv:1504.04025*
- Vogelsberger M., Zavala J., Loeb A., 2012, *MNRAS*, 423, 3740
- Vogelsberger M., Zavala J., Simpson C., Jenkins A., 2014, *MNRAS*, 444, 3684
- Wadsley J. W., Stadel J., Quinn T., 2004, *New Astronomy*, 9, 137
- Wadsley J. W., Veeravalli G., Couchman H. M. P., 2008, *MNRAS*, 387, 427
- Walker M. G., Peñarrubia J., 2011, *ApJ*, 742, 20
- Weisz D. R., Dolphin A. E., Skillman E. D., Holtzman J., Gilbert

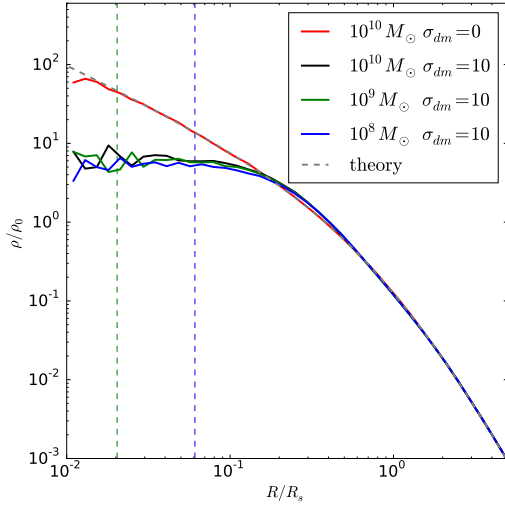


Figure 10. The density in scaled units of R/R_s for Hernquist halos of 10^{10} (black), 10^9 (green), and $10^8 M_\odot$ (blue) which have scale radii of 1.099, .37, and .12 Kpc respectively based on the mass concentration ratio from Neto et al 2007. Each halo has been evolved for about 25 scaled dynamical times which corresponds to 91, 44, and 20 million years respectively. The halos demonstrate self similar evolution in these scaled distance and time units. The density ρ has been scaled by the central density. The vertical dashed lines indicate the softening length of 7.5 pc that is scaled for each halo (the dashed line for the $10^{10} M_\odot$ halo is off the plot further to the left). The dashed grey dashed line is the Hernquist density profile.

K. M., Dalcanton J. J., Williams B. F., 2014, ArXiv 1405.3281
 Wolf J., Martinez G. D., Bullock J. S., Kaplinghat M., Geha M.,
 Muñoz R. R., Simon J. D., Avedo F. F., 2010, MNRAS, 406,
 1220
 Yoshida N., Springel V., White S. D. M., Tormen G., 2000, ApJ,
 544, L87
 Zavala J., Vogelsberger M., Walker M. G., 2013, MNRAS, L52
 Zolotov A. et al., 2012, ApJ, 761, 71

5 APPENDIX: THE SIDM IMPLEMENTATION

We verified our implementation of SIDM by comparing analytical predictions of the number of dark matter interactions to simulations of dark matter halos with a Hernquist density profile (Hernquist 1990) (Fig. 10). We then demonstrate the formation of a flat core and the signature flat SIDM velocity dispersion profile, starting from an NFW profile with a cuspy density profile and a raising velocity dispersion (Navarro et al. 1996). Our implementation code closely replicates published results of the predicted number of SIDM collisions as a function of halo mass and local density and the evolution of the central density profile (Vogelsberger et al. 2012; Rocha et al. 2013) (Fig.10 and Fig.11).

The number of dark matter interactions per unit time is an important cosmological value for SIDM theories and a useful diagnostic for numerical implementations of SIDM interactions. The probability of an interaction between any two particles is given in eq.4. The total number of interactions, Γ , that occur per unit time is

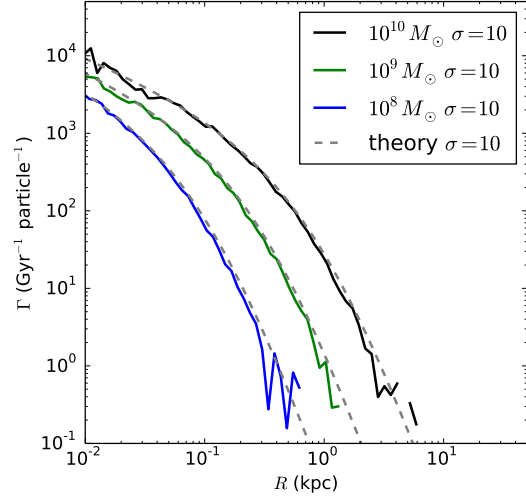


Figure 11. Snapshots of a Hernquist profile SIDM simulation showing the number of interactions that occur per particle per giga-year for the same halos as above. The cross section is $10 \text{ cm}^2 \text{ g}^{-1}$. In dashed grey is the analytical prediction for each halo respectively. The simulations were run for a period much shorter than the dynamical time of the halo. Each Hernquist profile has a different scaled structure as described in the previous figure. Each halo was described with about 2 million particles.

an integral of the velocity weighted cross section in the volume V .

$$\Gamma = \int \frac{\rho^2(\mathbf{x})}{2m_\chi} \langle \sigma_{dm} v_r \rangle(\mathbf{x}) dV \quad (3)$$

Where ρ is the local DM density, m_χ is the mass of the dark matter particles in the simulation, σ_{dm} is the dark matter cross section per gram, and $\langle \sigma_{dm} v_r \rangle(\mathbf{x})$ is the local thermal average of the cross section weighted by the particle's relative velocity as a function of the position \mathbf{x} . The local thermal average of the cross section is calculated by taking the first moment of $\sigma_{dm} v_r$ over the combined relative velocity distribution function $f(v_r)$.

$$\langle \sigma v_r \rangle(\mathbf{x}) = \int_0^\infty (\sigma_{dm} v_r)(\mathbf{x}) f(v_r) dv_r \quad (4)$$

In the most general case the distribution function can be a function of position (as for a dark matter halo) and the cross section can be a function of relative velocity (for velocity dependent SIDM). In the simplest case for single value initial velocity of v_0 and uniform density, the distribution function $f(v_r)$ becomes a delta function at that given velocity where $f(v_r) = \frac{\delta(|v|-v_0)}{4\pi v_0^2}$ and the interaction rate simplifies to $\Gamma = \sqrt{2}/2N\rho\sigma_{dm}v$ where N is the total number of dark matter particles in the simulation. A standard Maxwell-Boltzmann distribution has a constant velocity dispersion so that after averaging over all angles of collision we conclude $\langle v_r \rangle = \sqrt{2}\langle v \rangle$ so that if a is the standard deviation of the velocity vector in the distribution then the thermal average cross section is

$$\langle \sigma_{dm} v_r \rangle(\mathbf{x}) = \sqrt{2}\sigma_{dm} \sqrt{\frac{8a^2}{\pi}} \quad (5)$$

Thus in a constant density region with a Maxwell-Boltzmann ve-

locity distribution the number of interactions per unit time is

$$\Gamma = \frac{\sqrt{2}N\rho\sigma_{dm}}{2}\sqrt{\frac{8a^2}{\pi}} \quad (6)$$

We would like to have an analytic calculation for the number of interactions that would occur in a given dark matter halo, however in general the integrals of dark matter halos are not well behaved. Further, the dark matter interactions modify the density and velocity distribution of the halo by conducting energy (as a measure of velocity dispersion) from the outer regions of halo into the core. We approximate that after 25 scaled dynamical times $t_0^{-1} = \sigma_{dm}m_\chi R_s \sqrt{64G\rho_0^3}$ (where $\rho_0 = M/(2\pi R_s^3)$ is the central density) a core-collapse phase may start (Koda & Shapiro 2011). One well behaved halo profile is the Hernquist profile which has a dark matter density profile similar to an NFW profile. In figure 10 we show scaled Hernquist halos with masses of 10^{10} , 10^9 , and $10^8 M_\odot$ that have each been evolved for 25 scaled dynamical times. Under the assumption of an isotropic velocity distribution, the velocity dispersion σ_v of the Hernquist profile is known analytically from the literature and the average of $\langle\sigma_{dm}v_r\rangle(\mathbf{x})$ is then

$$\langle\sigma_{dm}v_r\rangle(\mathbf{x}) = \frac{1}{2\sqrt{\pi}\sigma_v^3(\mathbf{x})} \int_0^\infty (\sigma_{dm}v)v^2 \exp\left[-\frac{v^2}{4\sigma_v^2(\mathbf{x})}\right] dv \quad (7)$$

The total number of interactions per unit time is then given by equation 4 in the Appendix. However because the initial velocity dispersion is that of a Hernquist profile in equilibrium, this analytic prediction is an approximation which declines in accuracy with halo evolution in time. In figure 10 we show the analytic prediction of the expected number of DM interactions compared to a simulation of the halos that has been run for a brief period (10^5 years), much smaller than the dynamical time of the halos and before the density profile evolves significantly.

5.1 Convergence of SIDM profiles in DM-only simulations

In Figure 12 we show a resolution test using the most massive halo of simulation ‘h516’. The halo (of final mass $4 \times 10^{10} M_\odot$) was simulated lowering the mass resolution by a factor of 64 in mass and 4 in force resolution. The ratio of the spherically averaged local density as a function of radius show that the SIDM simulation converges at about 2 softening lengths, similar to the CDM run (see also Power et al. (2003)). The ‘central’ density decreases by a factor of ~ 6 between the CDM and SIDM case. These results agree with previous works. To verify the convergence of the SIDM density profiles at the previously poorly explored regime of $M_{vir} < 10^9 M_\odot$ we also simulated the ‘40 Thieves’ volume first with particle mass $8000 M_\odot$ and then again $2400 M_\odot$, and a force resolution of 65pc in both cases. Combining these runs with the h148 volume we are able to cover four orders of magnitude in halo mass, from small halos with peak velocities smaller than 10 km s^{-1} to massive galaxies with a large system of satellites. We have simulated h148 at lower resolution with hydrodynamics and SF, finding that it hosts a large disc galaxy.

This paper has been typeset from a \LaTeX file prepared by the author.

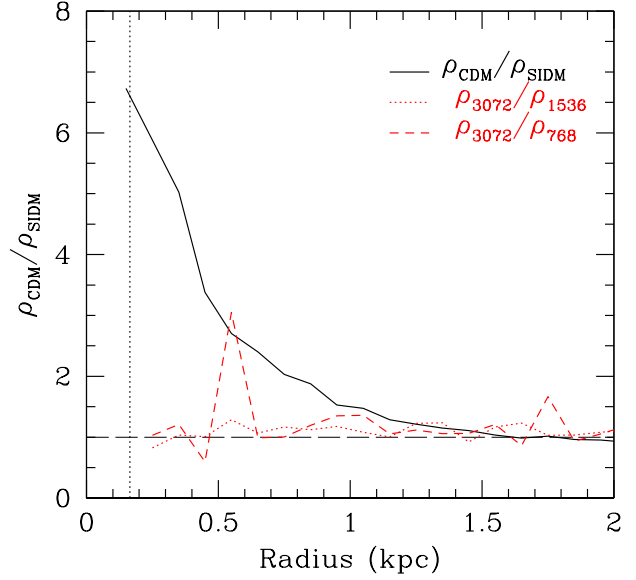


Figure 12. The local density ratio as a function of radius between the high resolution SIDM version of halo h516 (ρ_{SIDM}) and its lower resolution counterparts (ρ_{1536}) and (ρ_{768}). Results in the low res versions converge at \sim two softening lengths, as typical of CDM-only simulations.